PNAS

Supplementary Information for

Common activities and predictive gene signature identified for genetic hypomorphs of *TP53*

Jessica C. Leung, Julia I-Ju Leu, Alexandra M. Indeglia, Toshitha Kannan, Nicole A. Clarke, Nicole A. Kirven, Harsh Dweep, Thibaut Barnoud, Andrew V. Kossenkov, Donna L. George, Maureen E. Murphy

Maureen E. Murphy

Email: mmurphy@wistar.org

This PDF file includes:

Extended Methods

Mammalian cell culture. Human EBV-immortalized lymphoblastoid (LCL) cell lines were obtained from the Coriell Institute (Camden, New Jersey); for a complete list of LCL lines used, refer to **Table S1**. LCLs were cultured in RPMI 1640 supplemented with 15% fetal bovine serum, 1% penicillin/streptomycin, and 2 mM L-glutamine. Primary and transformed mouse embryonic fibroblasts (MEFs) were cultured in DMEM supplemented with 10% fetal bovine serum and 1% penicillin/streptomycin. Cells were grown in a 5% CO_2 humidified incubator at 37°C. All cell lines were confirmed to be free of mycoplasma prior to each experiment. WT, P47S, and Y107H primary mouse embryonic fibroblasts (MEF) were isolated from 13.5-day-old Hupki embryos and cultured at 37°C in DMEM with 1% penicillin/streptomycin and 10% FBS.

For the HCT116 P47S and Y107H cell lines, the P47S and Y107H point mutations were introduced respectively by nucleofection of HCT116 cells with a synthetic gRNA/Cas9 ribonucleoprotein complex along with a ssODN. The gRNA recognition site for P47S is 5'-ACCATTGTTCAATATCGTCC*NGG*, with the PAM site italicized, and the ssODN has the following sequence with two phosphorothioate bonds at each end: 5'-cttttcacccatctacagtccccttgccgtcccaagcaatggatgatttgatgctgtccAGTgacgatattgaacaatggttcactgaagaccc aggtccagatgaagctcccagaatg. The gRNA recognition site for Y107H is 5'- aaaacctaccagggcagctaCGG, with the PAM site in upper case, and the ssODN has the following sequence with two phosphorothioate bonds at each end: 5'-tgaccgtgcaagtcacagacttggctgtcccagaatgcaagaagcccagacggaaaccgtGGGAgccctggtaggttttctgggaaggg acagaagatgacaggggccaggaggggctggtgc. Both synthetic gRNAs and ssODNs in ultramer format were purchased from IDT. The transfected pools of HCT116 cells were analyzed by using Next Generation Sequencing for knock-in rate, and single-cell clones were obtained by sorting on a Sony sorter and screened by using Next Gen Sequencing. Positive clones were expanded, genotype confirmed prior to cryopreservation. All clones are negative for mycoplasma contamination and authenticated as HCT116

cells by STR profiling. P47S clones B5 (cl1) and G12 (cl2) and Y107H clones A11 (cl1) and C2 (cl2) were confirmed and the TP53 cDNA was sequenced in its entirety. Cells were treated with 10μM Nutlin-3a (Sigma-Aldrich) or 5μM CDDP (cisplatin; Med Chem Express) where indicated to induce p53 signaling. To assess NF-κB signaling, cells were treated with TNF-α (Sigma-Aldrich) at the indicated concentrations and time points. Prior to treatment with EGF (Sigma-Adrich), cells were serum starved in media supplemented with 1% fetal bovine serum for 6 hr.

For transient transfection of H1299 cells, cells were seeded at 1 x 10^6 cells in triplicate the day before transfection. Cells were transfected with pCMV3 empty vector or pCMV3 constructs containing the associated p53 mutation using Lipofectamine LTX and Plus Reagent for 24 hours. Media was replaced and cells were allowed to recover for an additional 24 hours before harvesting for western blot analysis.

Immunoblotting. For western blot analyses, 10-50 μg of protein was resolved over SDS-PAGE gels using 10% NuPAGE Bis-Tris precast gels (Life Technologies) and were then transferred onto PVDF membranes (pore size: 0.45mm; Millipore Sigma). Membranes were blocked for 1 hr in 5% bovine serum albumin or 5% non-fat dry milk. Membranes were then incubated overnight in primary antibody at 4°C while shaking. Rabbit or mouse secondary antibodies conjugated to horseradish peroxidase were used (Jackson ImmunoResearch), followed by a 5-min treatment with ECL. Protein levels were detected using autoradiography.

Antibodies. The following antibodies were used: anti-CEACAM1 (Invitrogen), anti-GAPDH (14C10; Cell Signaling Technology), anti-Histone H3 (acetyl K27; Abcam), anti-Histone H3 (acetyl K27; Abcam), anti-Hsc70 (Proteintech), anti-Ki67 (D3B5; Cell Signaling Technology), anti-LCN15 (Invitrogen), anti-Mdm2 (Cell Signaling Technology), anti-Mdm2 (Ab-1; Sigma-Aldrich), anti-Mdm2 (Ab-2; Sigma-Adrich), Mouse monoclonal IgG1 isotype control (G3A1; Cell Signaling Technology), anti-NF-κB p65 (D14E12; Cell Signaling Technology), anti-NF-κB p65 (phospho-Ser276; GeneTex), anti-p21 (12D1; Cell Signaling Technology), anti-p53 (1C12; Cell Signaling Technology), anti-p53 (7F5; Cell Signaling Technology), anti-p53 (CM5; Cell Signaling Technology), anti-p53 (DO-1; Santa Cruz Biotechnology),

anti-p53 (FL-393; Bioss), anti-p53 (mutant, pAb240; Santa Cruz Biotechnology), anti-PADI4 (GeneTex), anti-PUMA (Cell Signaling Technology), anti-RRAD (LSBio), and anti-TNF-α (GeneTex).

Immunoprecipitation. Tissues were homogenized using the Wheaton Overhead Stirrer in Lysis Buffer (50 mM Tris-HCl, pH 8; 150 mM NaCl, 5 mM EDTA, 0.5% IGEPAL CA-630) with freshly supplemented protease inhibitors at 4°C. Total cellular homogenates were rotated at 4°C for 30 min, and spun at 11,000 x g for 30 min at 4°C. Protein extracts (3 mg per reaction) were incubated with the anti-Hsc70 antibody (Proteintech) or control IgG overnight at 4˚C. The Hsc70-immunocomplexes were captured using the Recombinant Protein G Agarose (Thermo Fisher Scientific) at 4˚C for 2 h. The resins were washed three times using the Lysis Buffer. After adding an equal volume of 2x Laemmli Sample Buffer (BioRad**)** supplemented with 5% β-Mercaptoethanol (BioRad) to each reaction, the samples were heated for 10 min at 100°C. The Hsc70-associated proteins were size fractionated on Novex 4-20% Tris-Glycine Mini Protein Gels (Thermo Fisher Scientific) at room temperature and subsequently transferred overnight onto Immuno-Blot PVDF membranes (BioRad) at 4˚C. The membranes were blocked with 3% Blotting-Grade Blocker (BioRad) in 1X PBST for 30 min at room temperature and incubated with the anti-p53 antibody (Cell Signaling Technology) overnight at 4˚C. After washing the blots in 1X PBST, the membranes were incubated with Peroxidase AffiniPure $F(ab')_2$ Fragment Donkey Anti-Mouse IgG (H+L) (Jackson ImmunoResearch) at 1:10,000 dilution for 2 h at room temperature. Membrane-immobilized protein detection used ECL Western Blotting Detection Reagents (Cytiva RPN2106; MilliporeSigma).

Immunohistochemistry. Tissues were harvested and fixed in formalin overnight at 4°C, followed by a wash with 1X PBS and then placed in 70% ethanol prior to paraffin embedding. The Wistar Institute Histotechnology Facility performed the tissue embedding and sectioning. Paraffin embedded tissue sections were deparaffinized in xylene and rehydrated in ethanol (100%-95%-85%-75%) followed by distilled water. Samples underwent antigen retrieval by steaming slides in 10mM Citrate Buffer (pH 6). Endogenous peroxidase activity was quenched with 3% hydrogen peroxide and slides were incubated

in blocking buffer for 1 hr. The slides were incubated with primary antibody overnight at 4°C. Slides were washed with PBS and incubated with HRP-conjugated secondary antibody for 30 min. Antibody complexes were detected using DAB chromogen. Light counterstaining was done with hematoxylin. Slides were imaged on a Nikon 80i upright microscope and at least four fields were taken per section.

Immunofluorescence and proximity ligation assay. Cells were grown on eight-well chamber slides (Lab-Tek), and were treated with 5μM CDDP for 24 hr. Cells were fixed in 4% paraformaldehyde (Electron Microscopy Sciences) for 10 min, followed by 3 washes in 1X PBS and permeabilization with 0.25% Triton X-100 (Millipore Sigma) for 5 min. For immunofluorescence staining, cells were washed 3x with 1X PBS prior to blocking for 1 hr at room temperature in a blocking buffer consisting of 4% normal goat serum (Jackson Immunoresearch) and 1% bovine serum albumin in PBS. Cells were incubated overnight at 4°C with primary antibodies diluted in blocking buffer. Cells were washed 3x with 1X PBS and incubated with the following secondary antibodies at room temperature for 1 hr: Alexa Fluor 488 AffiniPure Goat anti-Mouse IgG (Jackson ImmunoResearch) and Alexa Fluor 594 AffiniPure Goat anti-Rabbit IgG (Jackson ImmunoResearch). Cells were mounted with media containing DAPI and images were captured using a Nikon TiE automated inverted microscope. Protein-protein interactions were assessed using the PLA Duolink in situ starter kit (Sigma-Aldrich) following the manufacturer's protocol. Images were captured using a Leica TSC SP5 confocal microscope.

BMH cross-linking. Human LCL cell lines were cultured in DMEM-high glucose supplemented with 10% FBS and 1X penicillin/streptomycin prior to beginning the assay. Cells were transferred to DMEM-high glucose without glutamine, methionine, and cystine, supplemented with freshly added 1% FBS, 1X penicillin/streptomycin, 0.1 mM L-Methionine, 0.5 mM L-Glutamine, and 0.033 mM – 0.1mM L-cystine for up to 24h. Where appropriate, cells were treated with 1 μg/mL arsenic trioxide (ATO; Sigma-Aldrich) overnight. Cells were harvested and cell pellets were resuspended in ice-cold 1X DPBS with 0.5% IGEPAL CA-630 containing freshly added protease inhibitors (1mM PMSF, 10 μg/mL Aprotinin, and 10 μg/mL Leupeptin). Samples were lysed by sonication. Lysates were treated with 1mM BMH and

incubated at 30°C for 30 min. Reactions were quenched with 2X Laemmli sample buffer with freshly added 10% 2-mercaptoethanol and then analyzed by immunoblotting.

In vitro invasion assays. Matrigel invasion assays for MEFs and HCT116 cells were carried out with 24-well BioCoat Matrigel Invasion Chambers with 8.0 μm PET membrane (Corning). In brief, chambers were rehydrated with serum free media and incubated for 2 h at 37 °C and then inserted into a 24-well filled with 750μL media supplemented with 10% FBS. Approximately 20,000-50,000 cells were seeded in the upper chamber in 500μL media supplemented with 1% FBS. Cells were allowed to adhere to the Matrigel prior to treating with 20 ng/mL TNFα, and were then incubated at 37 °C. After 24-30 h, cells that had not migrated into the Matrigel were removed from the upper surface of the membrane with a cotton swab. Inserts were fixed with 100% methanol, stained with 0.5% crystal violet, and imaged for analysis using a Nikon TE2000 Inverted Microscope. Number of invaded cells per field (n = 5 random fields of view per insert) were quantified with ImageJ (1.53j, NIH) and expressed as mean ± SD. Data are representative of two biological replicates.

RNA isolation and quantitative RT-PCR. Cells were lysed using QIAshredder columns (Qiagen). Total RNA was extracted using the RNeasy Mini kit (Qiagen) and on-column DNase digestions, according to the manufacturer's protocol. Equal amounts of total RNA were then used to generate cDNA using the High-Capacity Reverse Transcription kit (Applied Biosystems) according to the manufacturer's protocol. The resulting cDNA was used with PowerUp SYBR Green Master Mix and the indicated primer sets (see **Table S2**). Quantitative RT-PCR (Q-RT-PCR) was performed using the QuantStudio 5 Real-Time PCR System (Applied Biosystems). Ct values for the genes of interest were normalized to the invariant control genes. Gene expression data are expressed as relative quantity and normalized to untreated- or vehicle-treated WT controls. All experiments were replicated in at least three independent experiments with three technical replicates in each experiment unless otherwise stated.

Nuclear fractionation and sequential salt extraction. Cells were harvested and washed twice with ice cold PBS prior to resuspending in Buffer A (25mM HEPES pH 7.6, 25mM KCl, 5mM $MgCl_2$, 0.05mM

EDTA, 0.1% NP-40, 10% glycerol) supplemented with protease inhibitors. Cells were rotated at 4°C for 10 min and then centrifuged at 6000 x g for 5 min at 4°C to isolate nuclei. Each nuclear pellet was resuspended and homogenized in mRIPA (100mM Tris pH 8.0, 2% NP-40, 0.5% sodium deoxycholate), incubated on ice for 3 min, and then centrifuged at 6500 x g for 3 min at 4°C to isolate the chromatin pellet. The supernatant (soluble nuclear fraction) was transferred to a clean tube before proceeding with sequential salt extraction of the chromatin pellet. Each chromatin pellet was resuspended and homogenized in mRIPA with sequentially increasing concentrations of NaCl (100mM – 500mM), incubated on ice for 3 min, and centrifuged at 6500 x g for 3 min at 4°C to extract chromatin bound proteins. NuPAGE Sample Buffer (supplemented with 5% β-mercaptoethanol) was added to each fraction. Samples were loaded into an SDS-PAGE gel for western blot analysis.

Chromatin immunoprecipitation-quantitative PCR. LCLs (2.0×10^7) were treated with vehicle control or 0.5 ng/mL TNF-α for the indicated timepoints and then crosslinked with 1% formaldehyde for 10 minutes at room temperature and quenched with 2.5 M glycine for 5 minutes. Crosslinked cells were washed twice in PBS, collected by centrifugation, lysed in 10 ml swelling buffer (10 mM Tris, pH 7.5, 2 mM $MgCl_2$, 3 mM $CaCl_2$), and placed on ice for 10 minutes. Chromatin fragmentation was performed with a Bioruptor sonication bath (Diagenode) at 4 °C with the following settings: 25 cycles of high amplitude for 30 seconds, with a 30 second pause in between each sonication. Chromatin was then cleared with centrifugation at maximum speed for 30 minutes at 4 °C, 5% saved for input, and immunoprecipitated with the appropriate antibodies overnight at 4 °C using magnetic Dynabeads Protein G beads (ThermoFisher). Beads were subsequently subjected to the following washes: 2x5 min in ChIP-buffer (50 mM HEPES, pH 7.5, 155 mM NaCl, 1.1% Triton X-100, 0.11% NaDeoxycholate, 1 mM EDTA), 5 min in ChIP-buffer with an additional 500 nM NaCl, 5 min in TE buffer (10mM Tris-HCl pH 8.0, 1mM EDTA). The crosslink was reversed overnight at 65 °C with elution buffer (50 mM Tris-HCl pH 8.0, 10 mM EDTA, 1% SDS) before treatment with 0.33 mg/ml RNase A (ThermoFisher) and 0.5 mg/ml Proteinase K (Thermo) at 37°C for 2 h. DNA was isolated with phenol/chloroform followed by overnight ethanol precipitation at −20 °C. Q-RT-PCR was used to determine the enrichment of

immunoprecipitated DNA relative to the input DNA using gene-specific primer sets to the specified regions (see **Table S2**). Primers directed to a gene-desert were used as a negative control. ChIP–Q-RT-PCR experiments were performed in two independent biological replicates.

Bulk RNA-Seq Analysis

RNA-Seq data from the first experiment studied the effect of Nutlin in LCLs from individuals with P47S and Y107H was aligned using STAR (1) against hg19 version of human genome and RSEM (2) was used for estimation of read counts and FPKM values using Ensemble transcriptome information. DESeq2 package (3) was used for normalization and differential expression analysis. For the RNA-Seq experiment to identify a p53 hypomorph gene signature, the samples in triplicates or duplicates were assayed among three runs with the same two samples (one hypomorph and one wild-type) repeated among the runs. Alignment was done using bowtie2 (4) against hg19 version of human genome and Ensemble transcriptome information followed by RSEM to estimate read counts on gene level. Normalization was carried out using DESeq2 (3) and batch correction was performed using the two samples that were repeated in each of the 3 runs. Python's sci-kit learn (sklearn v0.24.2) (5) was used to train the SVM with an RBF kernel with leave-one-out (LOO) cross validation and recursive feature elimination (RFE) to select features based on the training set (6). The best 2000 genes based on t-test on log2-scaled normalized counts were used in each iteration of LOO and RFE was applied removing 10% of features with the lowest SVM scores at each step with the model retrained and the left-out group classified to produce a probability classification score. Probability scores were used to calculate accuracy using 0.5 threshold and area under the ROC curve. The optimal number of genes were selected based on highest accuracy and AUC of the training set. RFE iteration with 32-gene model showed the highest accuracy and AUC with a total of 143 unique genes across all steps of LOO iterations. The SVM was re-trained on the training set with these 143 genes and applied on a set of blinded samples from 6 patients. R package ggplot2 v3.3.5 was used for plotting graphs and figures. Qiagen Ingenuity Pathway Analysis (IPA) was used for enrichment analyses of genesets (7). The RNA-

seq data was deposited to the NCBI GEO database, and can be found under accession number GSE209837.

Mouse Models. All mice were of the C57Bl/6J strain. WT and P47S mice were generated previously in the humanized p53 knock-in backbone (Hupki) (8). Y107H Hupki mice were generated by micro-injection of Cas9/gRNA ribonucleoprotein complex along with single-stranded oligo deoxyribonucleotide donor (ssODN) into single-cell embryos of WT-Hupki mice in the Transgenic Facility at the Fox Chase Cancer Center. The gRNA recognition site is aaaacctaccagggcagctaCGG, with the PAM site in upper case. The ssODN has the following sequence: tgaccgtgcaagtcacagacttggctgtcccagaatgcaagaagcccagacggaaaccgtGGGAgccctggtaggttttctgggaaggg acagaagatgacaggggccaggaggggctggtgc. The single-piece synthetic gRNA and ssODN containing two phosphorothioate bonds at each end were ordered from Integrated DNA Technologies and validated in human K562 cells prior to microinjection for efficient introduction of the Y107H mutation. Two independent founders with heterozygous T to C mutations were bred to homozygosity and crossed to C57Bl/6 background for five generations. The entire p53 coding region was amplified and sequenced by the Genomics Facility at the Wistar Institute.

Preclinical analyses. All animal studies were completed in accordance with the recommendations in the Guide for the Care and Use of Laboratory Animals of the NIH. All protocols were approved by The Wistar Institute Institutional Animal Care and Use Committee (IACUC). Mice were housed in plastic cages with ad libitum diet and maintained with a 12 hr dark/12 hr light cycle at 22°C. For *in vivo* induced chronic colitis assays, 8- to 10-week-old male and female mice were administered 2% dextran sulfate sodium (DSS; Alfa Aesar) in three 4-day cycles separated by 17-day intervals. Mice were monitored three times per week for overall weight, stool consistency, and gross bleeding. Inflammatory score assessment was conducted in blinded manner by a pathologist (D. Garlick, StageBio).

Statistical analyses. Unless otherwise specified, all experiments were performed in three independent biological replicates and data were analyzed using the two-tailed unpaired t-test. All in vitro data are

reported as the mean ± SD unless stated otherwise. For data containing more than 2 experimental groups, one-way ANOVA with Tukey's post-test analysis was performed. All statistical analyses were performed in GraphPad Prism (v9.0).

Figure S1

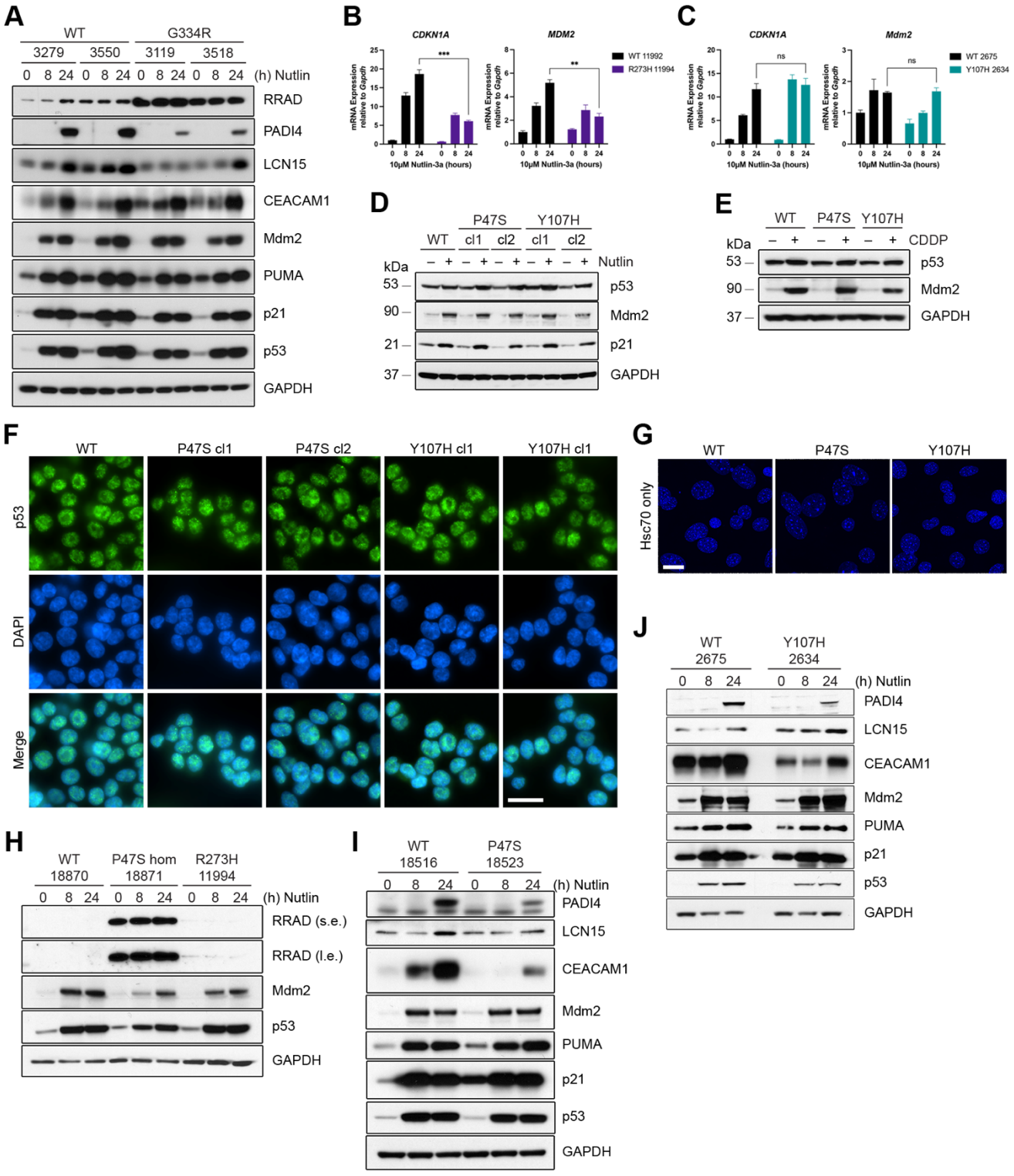
A
WT
G334R
3279
3550
3119
3518
0 8 24 0 8 24 0 8 24 0 8 24 (h) Nutlin
RRAD
PADI4
LCN15
CEACAM1
Mdm2
PUMA
p21
p53
GAPDH
B
CDKN1A
MDM2
mRNA Expression relative to Gapdh
10μM Nutlin-3a (hours)
WT 11992
R273H 11994
C
CDKN1A
Mdm2
ns
WT 2675
Y107H 2634
D
P47S
Y107H
WT
cl1
cl2
cl1
cl2
kDa
– + – + – + – + – + Nutlin
53
90
21
37
p53
Mdm2
p21
GAPDH
E
WT
P47S
Y107H
kDa
– + – + – + CDDP
53
90
37
p53
Mdm2
GAPDH
F
WT
P47S cl1
P47S cl2
Y107H cl1
Y107H cl1
p53
DAPI
Merge
G
WT
P47S
Y107H
Hsc70 only
J
WT
2675
Y107H
2634
0 8 24 0 8 24 (h) Nutlin
PADI4
LCN15
CEACAM1
Mdm2
PUMA
p21
p53
GAPDH
H
WT
18870
P47S hom
18871
R273H
11994
0 8 24 0 8 24 0 8 24 (h) Nutlin
RRAD (s.e.)
RRAD (l.e.)
Mdm2
p53
GAPDH
I
WT
18516
P47S
18523
0 8 24 0 8 24 (h) Nutlin
PADI4
LCN15
CEACAM1
Mdm2
PUMA
p21
p53
GAPDH

Fig. S1. Expression of p53 target genes and p53 protein conformation in hypomorphic cell lines

(*A*) Western blot analysis of WT or G334R LCLs treated with 10μM Nutlin-3a for the indicated time points. (*B-C*) WT and R273H (*B*) and WT and Y107H (*C*) LCLs were treated with 10 μM Nutlin-3a for the indicated time periods and analyzed by Q-RT-PCR with primers specific for *Cdkn1a* and *Mdm2* mRNA. Values were normalized for *GAPDH* mRNA as an internal control. Data are presented as mean ± SD. *n* = 3 technical replicates from 2 independent experiments. n.s. not significant; $^{**}p < 0.01$; $^{***}p < 0.001$ by one-way ANOVA followed by Šídák's multiple comparisons test. (*D*) Western blot analysis of WT, P47S, and Y107H HCT116 cells treated with 10μM Nutlin-3a for 24 hr. (*E*) Western blot analysis of WT, P47S, and Y107H primary MEFs treated with 5μM CDDP for 24 hr. (*F*) WT, P47S, and Y107H HCT116 cells stained with the pan-p53 (1C12) antibody confirmed equivalent total p53 expression by immunofluorescence analysis. Scale bar, 25μm. (*G*) Representative images of single antibody (Hsp70) conditions for WT, P47S, and Y107H primary MEFs, which served as a negative control for proximity ligation assay analysis. Scale bar, 20μm. (*H*) Western blot analysis of WT, P47S (homozygous), or R273H LCLs treated with 10μM Nutlin-3a for the indicated time points. s.e., short exposure; l.e., long exposure. (*I-J*) Western blot analysis of WT, (*I*) P47S, and (*J*) Y107H LCLs treated with 10μM Nutlin-3a for the indicated time points.

Figure S2

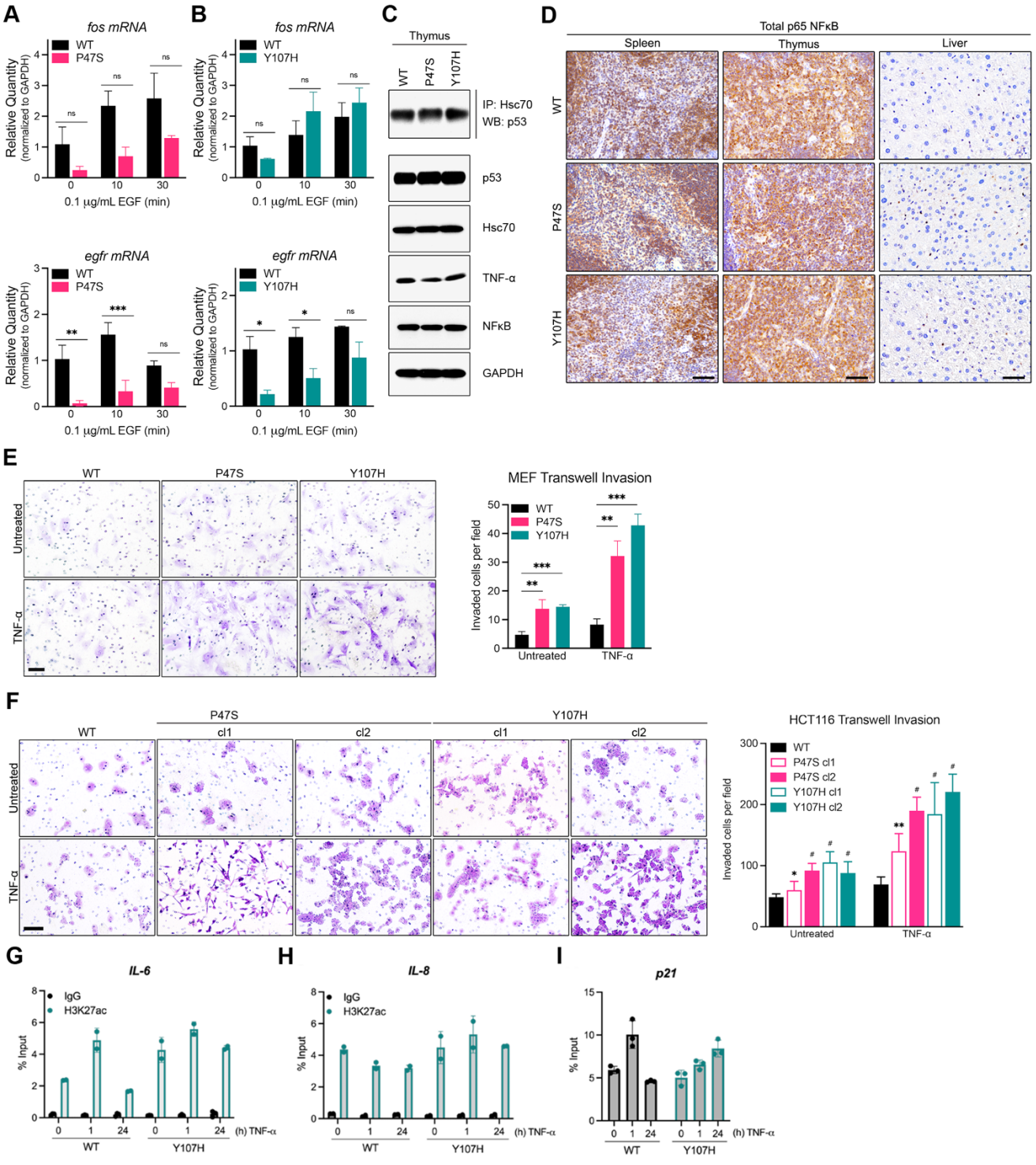

Fig. S2. p53 hypomorph response to stimulation by EGF and TNF-α

(*A-B*) WT, (*A*) P47S, and (*B*) Y107H LCLs were treated with 0.1 μg/mL EGF for the indicated time periods and analyzed by Q-RT-PCR with primers specific for *fos* and *egfr* mRNA. Values were normalized for *GAPDH* mRNA

as an internal control. Data are presented as mean ± SD. *n* = 6 technical replicates from 2 independent experiments. $^{*}p < 0.05$; $^{**}p < 0.01$; $^{***}p < 0.001$ by one-way ANOVA followed by Šídák's multiple comparisons test. (*C*) Hsc70 IP in thymus tissue harvested from 10 week old male mice of the indicated genotypes. Immunoprecipitation of Hsc70 or IgG negative control was followed by immunoblotting for p53 (left). Whole cell lysates were analyzed by western blotting with the indicated antibodies (right). (*D*) Representative immunohistochemical images of spleen, thymus, and liver sections obtained from ten week old male mice of the indicated genotypes. Tissue sections were stained for total p65 NF-κB. Scale bar, 50μm. (*E*) Representative images of crystal violet staining following Matrigel chamber invasion assays with primary MEFs (scale bar, 100 μm). Cells were treated with 20 ng/mL TNF-α for 24 hr. Quantification of the average number of invaded cells per condition; values are expressed as mean ± SD. n = 5 random fields of view from each of 3 biological replicates. $^{**}p < 0.01$; $^{***}p < 0.001$ as determined by two-tailed Student's t-test. (*F*) Representative images of crystal violet staining following Matrigel chamber invasion assays with HCT116 cells, treated with 20 ng/mL TNF-α for 30 hr (scale bar, 100 μm). Quantification of the average number of invaded cells per condition; values are expressed as mean ± SD. n = 5 random fields of view from each of 2 biological replicates. $^{**}p < 0.01$; $^{\#}p < 0.0001$ as determined by two-tailed Student's t-test. (*G-I*) WT and Y107H LCLs were treated with 0.5 ng/mL TNF-α for 0, 1, or 24h and subjected to ChIP with (*G-H*) IgG, H3K27ac, or (*I*) p53 antibodies, followed by Q-RT-PCR analysis with primers specific to the NF-κB site of the (*G*) *IL-6* and (*H*) *IL-8* promoters, as well as the (*I*) p53 site of the *p21* promoter. Values are presented as percentage of input. Error bars represent ± SD. $^{*}p < 0.05$; $^{**}p < 0.01$; $^{***}p < 0.001$ as determined by two-tailed Student's t-test.

Figure S3

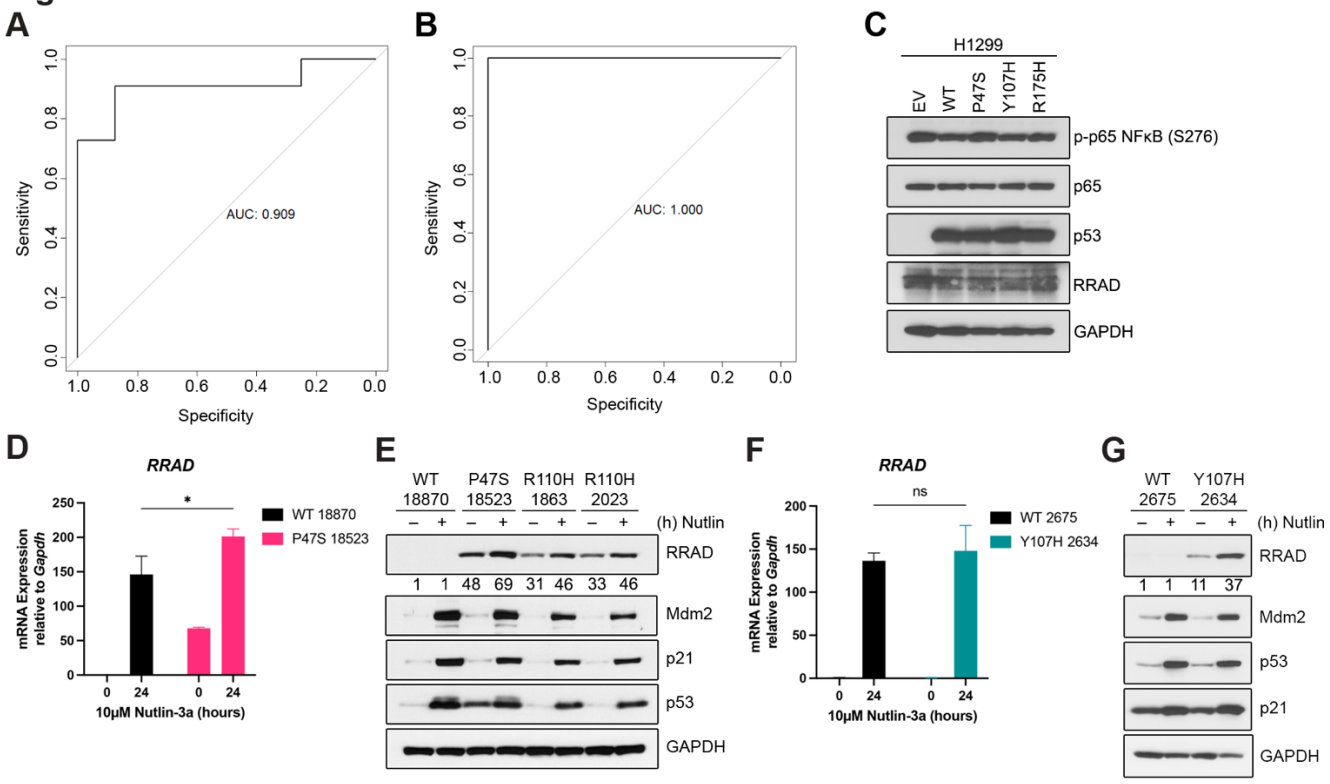

Fig. S3. Predictive p53 hypomorph gene signature and RRAD expression in benign and presumed hypomorphic p53 cell lines

(*A*) ROC AUC for Fig. 4A. (*B*) ROC AUC for Fig. 4B. (*C*) Western blot analysis of H1299 cells transfected with CMV vector (EV), WT p53, or expression constructs containing the P47S, Y107H, or R175H of p53. (*D*) WT and P47S LCLs were treated with 10μM Nutlin-3a for the indicated time periods and analyzed by Q-RT-PCR with primers specific for *Rrad* mRNA. Values were normalized for *GAPDH* mRNA as an internal control. Data are presented as mean ± SD. *n* = 3 technical replicates from 2 independent experiments. $^{*}p < 0.05$ by one-way ANOVA followed by Šídák's multiple comparisons test. (*E*) Western blot analysis of WT, P47S, or R110H LCLs treated with 10μM Nutlin-3a for 24 hr. (*F*) WT and Y107H LCLs were treated with 10μM Nutlin-3a for the indicated time periods and analyzed by Q-RT-PCR with primers specific for *Rrad* mRNA. Values were normalized for *GAPDH* mRNA as an internal control. Data are presented as mean ± SD. *n* = 3 technical replicates from 2 independent experiments. n.s. not significant; by one-way ANOVA followed by Šídák's multiple comparisons test. (*G*) Western blot analysis of WT and Y107H LCLs treated with 10μM Nutlin-3a for 24 hr.

Figure S4

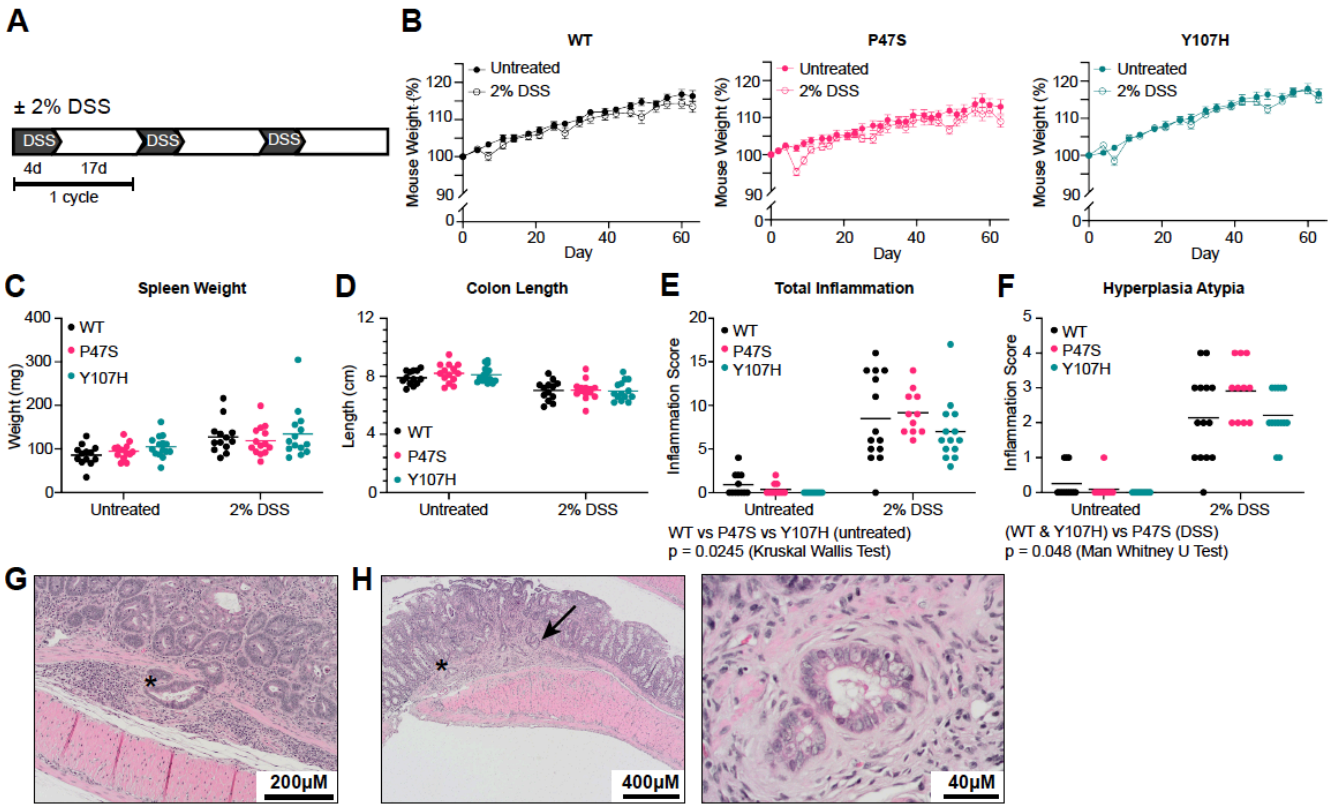

Fig. S4. P47S mice are sensitive to DSS-induced chronic inflammation

(*A*) Schematic detailing the treatment schedule for inducing chronic inflammation in WT, P47S, and Y107H mice by administering three cycles of DSS. (*B*) Mouse weights recorded throughout the study for both untreated mice and mice exposed to 2% DSS for each genotype. (*C-D*) At the conclusion of the study, (*C*) spleen weight and (*D*) colon lengths were measured as proximal analyses of inflammation response to DSS treatment. (*E-F*) Colonic inflammation was assessed by histopathological analysis; (*E*) total inflammation score and (*F*) hyperplasia atypia scores are reported. (*G-H*) Representative images of colon tissues in P47S mice demonstrating observed instances of (*G*) reactive hyperplasia reminiscent of colitis profunda (asterisk), as well as (*H*) extension into the submucosa (asterisk) and fibrotic reaction (arrow; higher magnification image, right). *n* = 6-8 mice per gender per treatment group; all analyses represent pooled data for both male and female mice.

Table S1. B lymphoblastoid cell lines

Cell Line/Classification	Source	Classifier
B Lymphocytes – G334R	(2)	3119
B Lymphocytes – WT	(2)	3279
B Lymphocytes – G334R	(2)	3518
B Lymphocytes – WT	(2)	3550
B Lymphocytes – WT	Coriell Institute	GM11992
B Lymphocytes – R273H	Coriell Institute	GM11994
B Lymphocytes – WT	Coriell Institute	GM18516
B Lymphocytes – Y220H	Coriell Institute	GM18519
B Lymphocytes – P47S	Coriell Institute	GM18523
B Lymphocytes – WT	Coriell Institute	GM18870
B Lymphocytes – P47S homozygote	Coriell Institute	GM18871
B Lymphocytes – E11Q	Coriell Institute	GM18954
B Lymphocytes – P47S	Coriell Institute	GM19092
B Lymphocytes – WT	Coriell Institute	GM19131
B Lymphocytes – P47S	Coriell Institute	GM19143
B Lymphocytes – P47S	Coriell Institute	GM19393
B Lymphocytes – WT	Coriell Institute	GM19394
B Lymphocytes – P47S	Coriell Institute	GM19982
B Lymphocytes – WT	Coriell Institute	GM19984
B Lymphocytes – G360A	Coriell Institute	GM20812
B Lymphocytes – WT	Coriell Institute	GM20814
B Lymphocytes – R110H	Coriell Institute	HG01863
B Lymphocytes – R110H	Coriell Institute	HG02023
B Lymphocytes – R110H	Coriell Institute	HG02085
B Lymphocytes – Y107H	Coriell Institute	HG02634
B Lymphocytes – WT	Coriell Institute	HG02675

B Lymphocytes – P47S	Coriell Institute	HG03297
B Lymphocytes – WT	Coriell Institute	HG03300
B Lymphocytes – WT	Coriell Institute	HG03753
B Lymphocytes – R175C	Coriell Institute	HG03755

NOTE: All p53 SNPs are heterozygous unless otherwise noted.

Table S2. Oligonucleotides for Real-time and ChIP quantitative PCR.

Target	**Forward primer**	**Reverse Primer**
Primers for Real-time qPCR		
Human *IL-6*	AAATTCGGTACATCCTCGACGGCA	AGTGCCTCTTTGCTGCTTTCACAC
Human *IL-8*	ATGACTTCCAAGCTGGCCGT	TCCTTGGCAAAACTGCACCT
Human *Fos*	CCTACCCGCCACGATGATGT	CTGCGGGTGAGTGGTAGTAA
Human *EGFR*	ACCTGACCGCAGAGTCTTTT	GAGTGGTTTGGCTGGGGTAA
Human *CDKN1A*	AGTCAGTTCCTTGTGGAGCC	GACATGGCGCCTCCTCTG
Human *MDM2*	CCCGGATTAGTGCGTACGAG	ATTGCACATTTGCCTGCTCC
Human *RRAD*	GCGGAAACCCTAAAGTCCGA	GTCCGGGACCGTCCACTC
Human *GAPDH*	TCGGAGTCAACGGATTTGGT	TTCCCGTTCTCAGCCTTGAC
Primers for ChIP qPCR		
Human *IL-6*	AGACATGCCAAAGTGCTGAGT	GAGGCTAGCGCTAAGAAGCA
Human *IL-8*	TGGGCCATCAGTTGCAAA	ACTTATGCACCCTCATCTTTTCAT
Human *p21*	AGCAGGCTGTGGCTCTGATT	CAAAATAGCCACCAGCCTCTTCT
Human desert	CATCCCTGGACTGATTGTCA	GGTTGGCCAGGTACATGTTT

SI References

1. Dobin A, Davis CA, Schlesinger F, Drenkow J, Zaleski C, Jha S, Batut P, Chaisson M, Gingeras TR. STAR: ultrafast universal RNA-seq aligner. Bioinformatics. 2013 Jan 1;29(1):15-21. doi: 10.1093/bioinformatics/bts635. Epub 2012 Oct 25. PMID: 23104886; PMCID: PMC3530905.

2. Li B, Dewey CN. RSEM: accurate transcript quantification from RNA-Seq data with or without a reference genome. BMC Bioinformatics. 2011 Aug 4;12:323. doi: 10.1186/1471-2105-12-323. PMID: 21816040; PMCID: PMC3163565.

3. Love MI, Huber W, Anders S. Moderated estimation of fold change and dispersion for RNA-seq data with DESeq2. Genome Biol. 2014;15(12):550. doi: 10.1186/s13059-014-0550-8. PMID: 25516281; PMCID: PMC4302049.

4. Langmead B, Salzberg SL. Fast gapped-read alignment with Bowtie 2. Nat Methods. 2012 Mar 4;9(4):357-9. doi: 10.1038/nmeth.1923. PMID: 22388286; PMCID: PMC3322381.

5. Pedregosa F., Varoquaux G., Gramfort A., Michel V., Thirion B., Grisel O., et al. (2011). Scikit-learn: machine learning in python. *J. Mach. Learn. Res*. 12, 2825

6. Cortes, C., Vapnik, V. Support-vector networks. *Mach Learn* **20,** 273–297 (1995). https://doi.org/10.1007/BF00994018

7. Krämer A, Green J, Pollard J Jr, Tugendreich S. Causal analysis approaches in Ingenuity Pathway Analysis. Bioinformatics. 2014 Feb 15;30(4):523-30. doi: 10.1093/bioinformatics/btt703. Epub 2013 Dec 13. PMID: 24336805; PMCID: PMC3928520.

8. Jennis M, Kung CP, Basu S, Budina-Kolomets A, Leu JI, Khaku S, Scott JP, Cai KQ, Campbell MR, Porter DK, Wang X, Bell DA, Li X, Garlick DS, Liu Q, Hollstein M, George DL, Murphy ME. An African-specific polymorphism in the TP53 gene impairs p53 tumor suppressor function in a mouse model. Genes Dev. 2016 Apr 15;30(8):918-30. doi: 10.1101/gad.275891.115. Epub 2016 Mar 31. PMID: 27034505; PMCID: PMC4840298.